ELSEVIER

Biophysical Chemistry 77 (1999) 27–35

Biophysical Chemistry

The apparently symmetrical hexagonal bilayer hemoglobin from *Lumbricus terrestris* has a large dipole moment[1]

Shiro Takashima[a,b], Askar R. Kuchumov[c], Serge N. Vinogradov[c,*]

[a] *Department of Bioengineering, University of Pennsylvania, Philadelphia, PA 19104, USA*
[b] *Biomedical Engineering Program, Drexel University, Philadelphia, PA 19104, USA*
[c] *Department of Biochemistry and Molecular Biology, Wayne State University School of Medicine, Detroit, MI 48201, USA*

Received 4 November 1998; accepted 16 November 1998

Abstract

The giant ~3.6 MDa hexagonal bilayer hemoglobin (HBL Hb) from *Lumbricus terrestris* consists of 12 213-kDa dodecamers of four globin chains ($[b + a + c]_3[d]_3$) tethered to a central scaffold of ~36 non-globin, linker subunits L1–L4 (24–32 kDa). Three-dimensional reconstructions obtained by electron cryomicroscopy showed it to have a D_6 point-group symmetry, with the two layers rotated ~16° relative to each other. Measurement of the dielectric constants of the Hb and the dodecamer over the frequency range 5–100 kHz indicated relaxation frequencies occurring at 20–40 and 300 kHz, respectively, substantially lower than the 700–800 kHz in HbA. The dipole moments calculated using Oncley's equation were $17\,300 \pm 2300$ D and 1400 D for the Hb and dodecamer, respectively. The approximately threefold higher dipole moment of the dodecamer relative to HbA is consistent with an asymmetric shape in solution suggested by small-angle X-ray scattering. Although a two-term Debye equation and a prolate ellipsoid of revolution model provided a good fit to the experimental dielectric dispersion of the dodecamer, a three-term Debye equation based on an oblate ellipsoid of revolution model was required to fit the asymmetric dielectric dispersion curve of the Hb: the required additional term may represent either an induced dipole moment or a substructure which rotates independently of the main permanent dipole component of the Hb. The D_6 point-group symmetry implies that the dipole moments of the dodecamers cancel out. Thus, in addition to a possible contribution from fluctuations of the proton distribution, the large dipole moment of the Hb may be due to an asymmetric distribution of the heterogeneous linker subunits.

Keywords: Dipole moment; Hemoglobin; Dodecamer subunit; *Lumbricus terrestris*

[1] This research was supported in part by NIH Grant DK 38674.
* Corresponding author. Tel.: +1 313 5771501, fax: +1 313 5772765, e-mail: svinogra@med.wayne.edu
Abbreviations: HBL, hexagonal bilayer; Hb, hemoglobin; Chl, chlorocruorin; EDTA, ethylenediaminetetraacetic acid; 3D, three-dimensional; cryoEM, cryoelectron microscopic; TEM, transmission electron microscopy; STEM, scanning transmission electron microscopy; ESI-MS, electrospray ionization mass spectrometry; SAXS, small-angle X-ray scattering

0301-4622/99/$ - see front matter
PII: S0301-4622(99)00006-X

1. Introduction

The HBL quarternary structure is characteristic of the giant extracellular Hbs of annelids (oligochaetes, leeches and polychaetes) living in terrestrial, aquatic and marine environments and in vestimentiferans and polychaete annelids which exist at the sulfide-rich hydrothermal vents on the Pacific Ocean floor at depths of 2500 m and whose subsistence in this hostile environment depends on symbiosis with sulfur-oxidizing prokaryotes [1]. The Hb from the common North American earthworm *Lumbricus terrestris* is the best studied of the HBL Hbs. It is comprised of four different globin chains (a–d, ~17 kDa), which occur as a disulfide bonded trimer T [a + b + c] and a monomer M (d) and four types (L1–L4) of non-globin linker subunits (24–32 kDa). Mild dissociation of the Hb established the principal functional subunit to be a 213 kDa dodecamer of globin chains, $[T]_3[M]_3 = [a + b + c]_3[d]_3$ [2], which was also shown to be an obligate intermediate not only in the dissociation but also in the reassembly of the Hb [3]. A 'bracelet' model of *Lumbricus* Hb proposed earlier [4], has been refined recently based on a detailed ESI-MS study to consist of 12 dodecamers tethered to a central 'bracelet' of 36 or 42 linker subunits [5]. 3D reconstructions of *Lumbricus* Hb based on cryoEM have provided a convincing demonstration of the essential correctness of this model [6,7]. Furthermore, concurrent 3D reconstructions of the Chl from the polychaete *Eudistylia* [8] and the Hbs from the leech *Macrobdella* [9] the vestimentiferan *Riftia* [10] and the deep sea polychaete *Alvinella* [11], have shown them to have essentially almost identical structures at the resolution achieved, ~30 Å. The quaternary structures of HBL Hbs and Chls in stained and unstained TEM and STEM images and in the 3D reconstructions obtained by cryoEM all have D_6 point-group symmetry. We report below a study of the dielectric properties of *Lumbricus* Hb and its dodecamer subunit, which shows the Hb to have a large dipole moment, in conflict with its apparent highly symmetric quaternary structure.

2. Experimental procedures

2.1. Materials

Lumbricus Hb and its dodecamer subunits, both in the oxy form, were prepared as discussed elsewhere [2,12]. The protein samples were dialyzed exhaustively against 1 mM EDTA in doubly distilled water. The dialysate was used as the reference solution and for the dilution of the sample.

2.2. Measurement of the dielectric constant of protein solutions

The general procedure was to measure sequentially the capacitances of the protein solution and an electrolyte solution (NaCl or KCl) having a similar conductance. The capacitance and conductance of the solution were measured using a Hewlett-Packard 4192A impedance analyzer which is fully automated using an on-line computer Macintosh Centris 650. The measurements were performed using a sampling program Labview 3, over the frequency range 5 kHz–10 MHz; the number of points sampled was usually 1000. The dielectric constant of the sample solution was calculated using Eq. (1) [13],

$$\varepsilon_S = 1 + \{(C_S - C_O)/(C_W - C_O)\}(\varepsilon_{H_2O} - 1) \quad (1)$$

where C_S is the capacitance of the sample solution, C_O is the capacitance of the empty cell, C_W is the capacitance of the NaCl or KCl solution with its conductance carefully adjusted to equal that of the protein sample and ε_{H_2O} is the dielectric constant of water, 78.5 at 25°C. The temperature of the sample and the reference solutions was maintained at 25°C using a Haake FK2 circulating thermostat. The concentrations of *Lumbricus* Hb and its dodecamer subunit were in the range of 1–20 mg/ml. The sampled data points were stored as spread sheets (Microsoft Excel version 4). The Excel program was used for all other data manipulations except plotting.

2.3. Analysis of the dielectric relaxation

The frequency dependence of the dielectric

constant of polar molecules can be represented using the Debye dispersion equation,

$$\varepsilon = \varepsilon_\infty + \Delta\varepsilon / \left[1 + (f/f_r)^2\right] \quad (2)$$

where ε is dielectric constant, f is the frequency of the applied field, f_r is the relaxation frequency and $\Delta\varepsilon$ is the dielectric increment, defined as the difference between the low- and high-frequency limiting dielectric constants, i.e. $\varepsilon_o - \varepsilon_\infty$ [14,15]. This equation holds for spherical molecules of uniform size with no dipolar interactions, where dielectric relaxation is characterized by only one time constant. Biological macromolecules in general do not satisfy these conditions [16–18] and, in particular, neither do *Lumbricus* Hb or its dodecamer subunit. Fig. 1 shows the 3D reconstruction volumes of the native Hb obtained by Lamy et al. [7]. The diameter and height of the Hb are known to be 30 and 20 nm, respectively, from previous TEM and STEM work [19]. The $[T]_3[M]_3$ dodecamer (indicated by the dotted circle in Fig. 1c), appears to have an umbrella-like shape with a diameter of approximately 11 nm and a height of 7 nm [20,21], with the three monomer M subunits clustering at the center, as observed recently in the 3D reconstruction of the reassembled HBL missing the M subunits [7]. We have tried to reproduce the shapes of the Hb and the dodecamer subunit using oblate and prolate ellipsoids of revolution, respectively, as shown diagrammatically in Fig. 2.

The dielectric dispersion data of *Lumbricus* Hb and its dodecamer subunit were analyzed using extended forms of Eq. (2),

$$\varepsilon = \Delta\varepsilon_\infty + \Sigma\Delta\varepsilon_j / \left[1 + (f/f_r)^2\right] \quad (3)$$

where j is either 2 or 3. Although this equation can also be written in an integral form or in the form of the Cole–Cole equation [22], we used the discrete form because of its convenience for the analysis of molecular shape. In addition, we normalized the dielectric increment $\Delta\varepsilon$, so that it ranges from 0 to 1, i.e. from $(\varepsilon - \varepsilon_\infty)$ to $(\varepsilon - \varepsilon_\infty)/\Delta\varepsilon$, where $\Delta\varepsilon = (\varepsilon_o - \varepsilon_\infty)$. For the two-term dispersion equation, the sum of the two increments is normalized, i.e. $\Delta\varepsilon_a + \Delta\varepsilon_b = 1$,

$$(\varepsilon_o - \varepsilon_\infty)/\Delta\varepsilon = \Delta\varepsilon_a / \left[1 + (f/f_a)^2\right] + (1 - \Delta\varepsilon_a) / \left[1 + (f/f_b)^2\right] \quad (4)$$

where f_a and f_b are the characteristic frequencies of orientation of the ellipsoid along the major and minor axes, respectively. The numerical factors f_a and f_b can be calculated from Perrin's equation [15,16,23,24], which uses orientation fac-

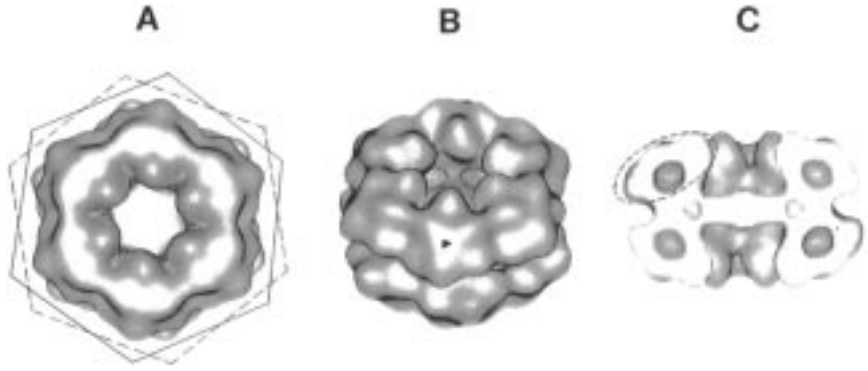

Fig. 1. Surface representations of the 3D reconstruction volume of *Lumbricus* Hb obtained by cryoEM at a resolution of ~35 Å (7). (a) Top view; (b) 45° view; (c) whole molecule cut in half by a plane passing through the sixfold axis. Note the following: (1) the top hexagonal layer of hollow globular substructures [HGS, marked by dotted circle in (c)] is rotated by ~16° relative to the lower layer; (2) each HGS has a local threefold axis of symmetry [indicated by triangle in (b)]. Each HGS is thought to consist of a dodecamer of globin chains which comprises the top portion [dashed oval in (c)] and non-globin linkers which comprise the bottom portion and also the central linker complex. Courtesy of Dr F. De Haas and Dr J. Lamy.

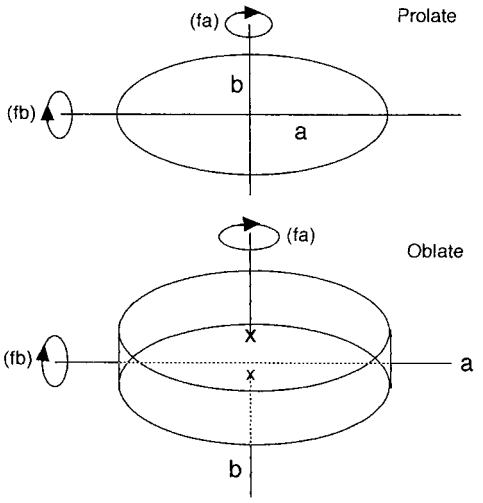

Fig. 2. Schematic diagram of the rotational modes of prolate and oblate ellipsoids.

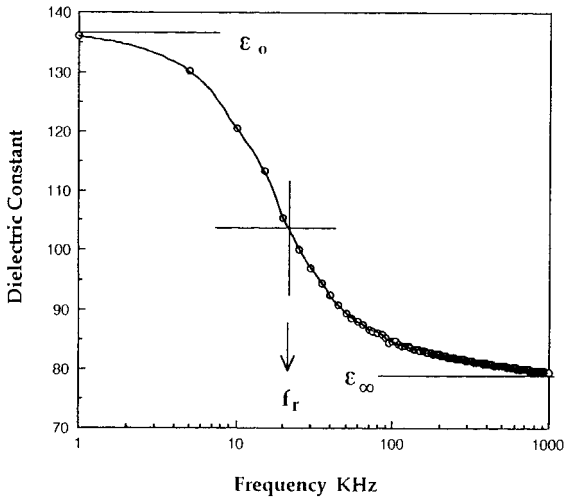

Fig. 3. The dielectric dispersion of *Lumbricus* Hb; ε_o and ε_∞ are the low- and high-frequency dielectric constants, respectively; f_r is the relaxation frequency. The circle at 1 kHz was inserted by manual extrapolation for the convenience of computer plotting.

tors f_o/f_a and f_o/f_b, where f_o is the characteristic frequency of an equivalent sphere, i.e. a sphere having the same volume as the ellipsoid. The numerical values of f_o/f_a and f_o/f_b calculated for various ratios of the two axes a and b are given in Appendix A.

3. Results

3.1. Dielectric dispersions of Lumbricus Hb and the dodecamer subunit

Figs. 3 and 4 show the dielectric dispersions, i.e. the frequency dependence of the dielectric constants, of *Lumbricus* Hb and the dodecamer subunit. The relaxation frequencies occurred in the range of 25–40 and 300 kHz, for the Hb and its subunit, respectively, unusually low compared to other globular proteins, such as human Hb, where it is found at 700–800 kHz [25].

3.2. Dipole moments of Lumbricus Hb and dodecamer subunit

The dipole moments of protein molecules are generally calculated using Oncley's equation [16],

$$\mu^2 = \{9000kTM/4\pi Nh\}\Delta\varepsilon/c \qquad (5)$$

where kT is the Boltzmann constant times the absolute temperature, M is the molecular weight, N is Avogadro's number and h is an empirical parameter, $\Delta\varepsilon$ is the dielectric increment and c is the concentration in g l^{-1}. Since $\Delta\varepsilon/c$ varies slightly with c, as shown in Fig. 5, the intrinsic dielectric increment at $c = 0$ was obtained either

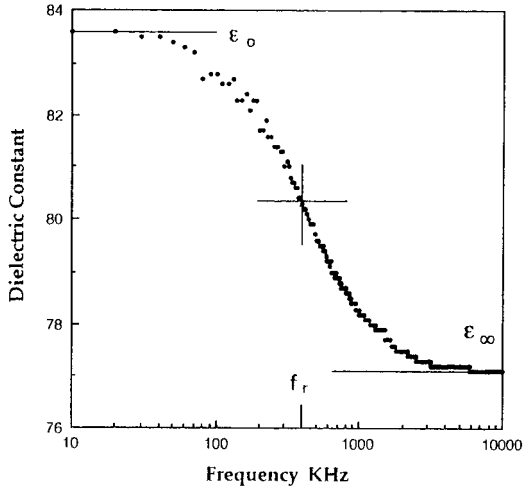

Fig. 4. The dielectric dispersion of the dodecamer subunit solution. The symbols are the same as in Fig. 3.

by extrapolation or from the slope of the plot of $\Delta\varepsilon$ vs. c. The dielectric dispersion measurement were performed using three different preparations of *Lumbricus* Hb; the dipole moments calculated using the intrinsic dielectric increment of 11.1 g^{-1} l^{-1} were 19 860 D, 15 200 D and 16 925 D, providing a mean value of 17 300 ± 2300 D (Table 1). The dipole moment of the dodecamer, calculated using the intrinsic dielectric increment of 0.85 g^{-1} l^{-1} and the molecular weight of 213 kDa and Eq. (4), was 1400 D (average of two measurements) (Table 1).

3.3. Prolate ellipsoid model of the dodecamer subunit

The value of f_o was estimated using the Stokes equation,

$$f_o = kT/6V\eta \quad (6)$$

where V is the volume of the molecule and η is the viscosity of water, i.e. 0.01 poise. Using the calculated volume of the dodecamer subunit (V = molecular weight/density/Avogadro's number), ~ 266 nm^3, which agrees with the 255 ± 10 nm^3 determined by SAXS [9], we obtain f_o = 145 kHz. Simulated dispersion curves were computed using Eq. (4) and letting $\Delta\varepsilon_a$ vary. The best fit with the experimental data was obtained for a/b = 2.5–3.0 and $\Delta\varepsilon_a$ = 0.45–0.55 (i.e. $\Delta\varepsilon_a/\Delta\varepsilon_b$ = 0.81–1.23) as shown in Fig. 6, where the solid line represents the calculated dispersion curve and the circles represent the experimental points. In addition, using the expression $\vartheta = \tan^{-1}(\Delta\varepsilon_a/\Delta\varepsilon_b)$, we calculated the angle between the dipole moment and molecular axes of the model to be approximately 39–51°, as well as the magnitudes of the transverse ($\mu_x = \mu \sin\vartheta$) and longitudinal ($\mu_y = \mu \cos\vartheta$) dipole moments. From the results shown in Table 2, it can be seen that the prolate ellipsoid model of the dodecamer suggests that it has equally large dipole moments along the major as well as the transverse axes, as shown schematically in Fig. 7.

Table 1
Dipole moments and relaxation frequencies of *Lumbricus* Hb, its dodecamer subunit and human HbA (1 D = 10^{-18} esu.cgs/cm)

Protein	Molecular mass (kDa)	Relaxation frequency (kHz)	Dipole moment (D)
Lumbricus Hb	3600	20–40	17 300 ± 2300
Dodecamer subunit	213	300	1400
Human HbA[a]	67	800–1000	485

[a] From Takashima [25].

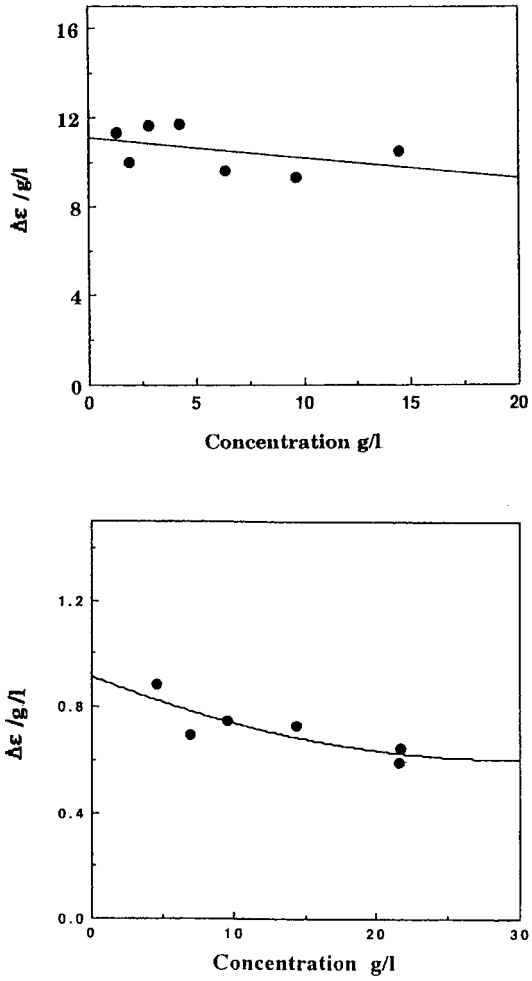

Fig. 5. Plots of the specific dielectric increment $\Delta\varepsilon/c$ vs. the concentration c in g l^{-1} for *Lumbricus* Hb (upper panel) and the dodecamer subunit (lower panel).

3.4. Oblate ellipsoid model of the Hb

The dielectric dispersion of the Hb shown in

Table 2
The variation in the transverse and longitudinal components of the dipole moment of the dodecamer subunit with the change in the angles between the dipole and molecular axes

$\varepsilon_a/\Delta\varepsilon_b$	Angle (ϑ)	Transverse component[a] (D)	Longitudinal component[a] (D)
0.45:0.55	39.3	889	1090
0.5:0.5	45.0	993	993

[a] The transverse and longitudinal components are given by $\mu_x = \mu \sin\vartheta$ and $\mu_y = \mu \cos\vartheta$, respectively.

Fig. 3 could not be fitted satisfactorily with a two-term Debye equation because it was asymmetric, the slope at low frequencies being steeper than at high frequencies. This asymmetry suggests the presence of an additional component rotating independently with a different, higher in this case, relaxation frequency. We used a three-term Debye equation, with the first two terms on the right-hand side identical to Eq. (6) and a third term, $\Delta\varepsilon_c/[1+(f/f_p)^2]$, representing a component rotating independently of the other two with a characteristic frequency f_p and subject only to the constraint that $\Delta\varepsilon_a + \Delta\varepsilon_b + \Delta\varepsilon_c = 1$. We assumed the additional component to have a spherical shape and a single relaxation time and used

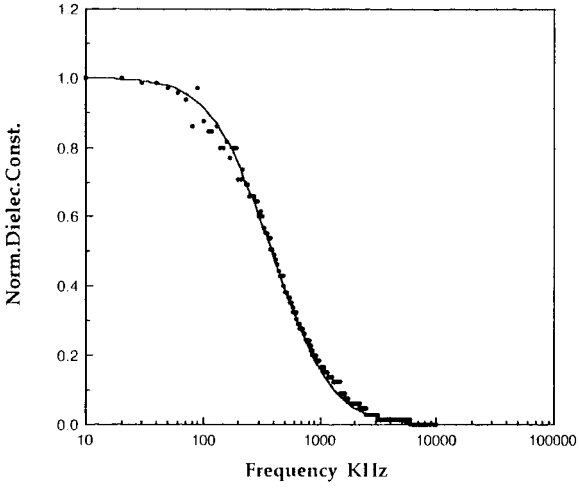

Fig. 6. A fit of the normalized dielectric dispersion of the dodecamer subunit to a prolate ellipsoid model using a two-term Debye dispersion equation with axial ratio $a/b = 3.5$ and $\Delta\varepsilon_a/\Delta\varepsilon_b = 0.5$.

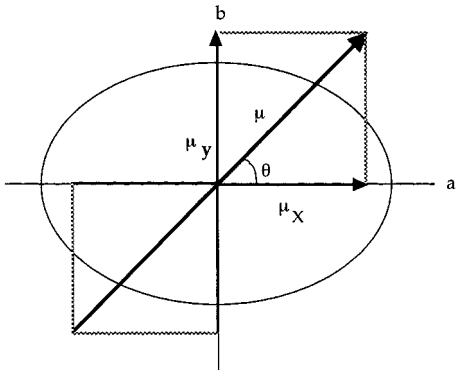

Fig. 7. A schematic representation of the dipole moments along the major and minor axes of the prolate ellipsoid of revolution model of the dodecamer subunit.

f_p as an adjustable parameter. Fig. 8 demonstrates that a satisfactory agreement was obtained between the experimental points and the calculated dispersion curve for $f_p = 180$–200 kHz and $\Delta\varepsilon_c \sim 0.1$.

4. Discussion

Investigations of the dipole moments of proteins undertaken by Oncley and his collaborators in the late 1930s [16], predate studies of protein structure. Since then, many proteins have been investigated using either by the frequency domain method [16,26] or the time domain method [27,28] and the experimental dipole moments compared with calculated values based upon crystallographic coordinate sets [25,29–31] for small proteins such as myoglobin and even hemoglobin. Except for a few cases, the agreement between the experimental and calculated dipole moments is satisfactory. A recent screening of some 500 protein crystal structures has revealed that the majority of the calculated dipole moments were in the range of several hundreds Debye units, with 46 proteins having dipole moments greater than 1000 D and only a few exceeding 2000 D [32]. Given the asymmetric, umbrella-like shape of the dodecamer in solution, suggested by SAXS measurements [9], with the three M subunits clustered in the center of the umbrella, evident from 3D reconstructions of cryoEM images of a reassembled HBL structure lacking the M subunits

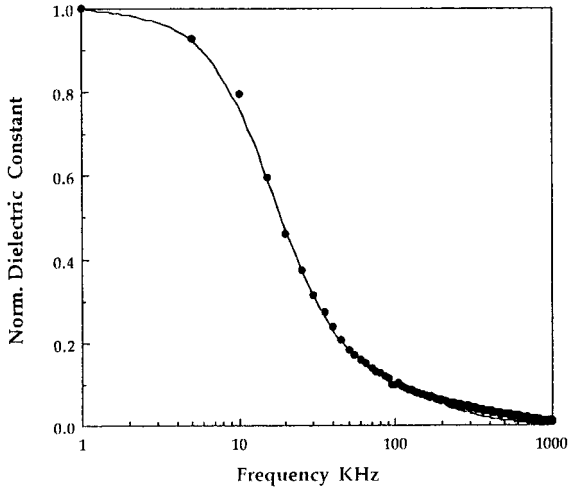

Fig. 8. A fit of the normalized dielectric dispersion of *Lumbricus* Hb to an oblate ellipsoid model using a three-term Debye equation, with axial ratio $a/b = 1.5$, $f_p = 180–200$ kHz and $\Delta\varepsilon_a:\Delta\varepsilon_b:\Delta\varepsilon_c = 0.2:0.7:0.1$.

[7], it is not surprising that the dodecamer has a dipole moment of 1400 D, approximately three times the dipole moment of HbA, 480–500 D [25] (Table 1). The very large dipole moment of the native Hb, 17300 D, would be easy to explain, if the dodecamers were aligned in one direction relative to the sixfold axis of the Hb. However, the 3D reconstruction obtained by cryoEM (Fig. 1) clearly shows the two rings of putative dodecamers to be oriented opposite to each other, in agreement with the absence of any aggregation of the native HBL Hb in solution. If we accept this fact, then even with the $\sim 16°$ rotation of the two layers (Fig. 1), the D_6 point-group symmetry would dictate the complete cancellation of the six vs. six dodecamer dipole moments. Thus, an explanation for the large dipole moment of the Hb must be sought elsewhere.

Early model calculations by Kirkwood and Shumaker [33] have suggested the possibility that fluctuations of the proton distribution in proteins could provide a substantial contribution to the measured dipole moment. Although this contribution in the case of proteins with a molecular weight of less than 100 kDa is probably too small to be observed [34], it may be substantial in the case of such a large multisubunit complex as *Lumbricus* Hb, consisting of some 144 globin chains and ~ 36 linker chains [5]. Since the induced dipole moment due to ion fluctuation is proportional to the square of the molecular radius, it is possible that for *Lumbricus* Hb which has a diameter of 30 nm, the induced dipole moment could be significant in contributing to the asymmetry of the experimental dielectric dispersion.

The linker subunits L1–L4 are known to be heterogeneous from detailed studies of the ESI mass spectra of the Hb [5] and of the isolated linkers (A.R. Kuchumov, J.A. Loo and S.N. Vinogradov, unpublished observations). Hence it is possible that an arrangement of linker subunits of slightly different primary structures with a symmetry lower than hexagonal could provide a permanent anisotropy of charge distribution responsible for the observed high dipole moment. Furthermore, the linkers have high affinity Ca^{2+} binding sites, due probably to the presence of ~ 40 amino acid residue-long cysteine-rich domains which are known to bind Ca^{2+} avidly [35,36] and in agreement with earlier experimental findings that complete removal of Ca^{2+} is impossible even upon complete dissociation of the native Hb [5]. Thus, in addition to the possible asymmetry of the linker subunit arrangement in the native *Lumbricus* Hb, there may occur states with asymmetric Ca^{2+} ion distributions which would also contribute to the overall charge distribution anisotropy. Single positive charges $(+1e)$ positioned diametrically opposite negative charges $(-1e)$ at distances of 20 nm and 30 nm, the height and diameter of *Lumbricus* Hb, will produce dipole moments of 1920 D and 2880 D, respectively. Thus, approximately 6–9 opposite charges located at the periphery of the HBL complex would account for the experimental dipole moment of 17300 D.

It should be noted that an experimentally observed, large permanent dipole moment in proteins with presumed symmetrical quaternary structures has been found to be a reliable indicator of asymmetric structure. A dipole moment of 1200 D determined by Porschke for the homotetrameric lac repressor [28] suggested an asymmetric structure, a conclusion which was verified by

the recently determined crystal structure [37,38]. Likewise, the Tet repressor also has a large dipole moment of 1050 D [39].

Appendix A

The orientation factors f_o/f_a and f_o/f_b are calculated using the following equations. For a prolate ellipsoid of revolution, the axial ratio $k = b/a$ ($a > b$), the Perrin equations are

$$f_o/f_a = 2(1-k^4)/\left\{\left[3k^2(2-k^2)/\sqrt{(1-k^2)}\right] \times \ln\left[\left(1+\sqrt{1-k^2}\right)/k\right] - 3k^2\right\}$$

for the orientation along the major axis a, and

$$f_o/f_b = 4(1-k^4)/-\left\{\left[3k^2(2k^2-1)/\sqrt{(1-k^2)}\right] \times \ln\left[\left(1+\sqrt{1-k^2}\right)/k\right] + 3\right\}$$

for the orientation around the minor axis b. The equations for oblate ellipsoids of revolution are

$$f_o/f_a = 2(1-k^2)/\left\{\left[3k^2(2-k^2)/\sqrt{(k^2-1)}\right] \times \left(\tan^{-1}\sqrt{k^2-1}\right) - 3k^2\right\}$$

for the orientation along the equatorial axis b, and

$$f_o/f_b = 4(1-k^4)/-\left\{[3k^2(2k^2-1)]/\sqrt{k^2-1} \times \left(\tan^{-1}\sqrt{k^2-1}\right) + 3\right\}$$

for the orientation around the axis of revolution a. The numerical values of Perrin's factors are given in the table below.

Table A1

Axial ratio a/b	Prolate ellipsoid		Oblate ellipsoid	
	f_o/f_a	f_o/f_b	f_o/f_a	f_o/f_b
0.667	1.192	1.006	1.013	1.100
0.5	1.505	1.050	1.132	1.256
0.4	1.892	1.095	1.289	1.358
0.333	2.344	1.134	1.464	1.578
0.286	2.852	1.165	1.651	1.791
0.25	3.395	1.189	2.002	1.843
0.2	4.641	1.226	2.240	2.423
0.167	6.065	1.250	2.442	2.843

References

[1] J.N. Lamy, B.N. Green, A. Toulmond, J.S. Wall, R.E. Weber, S.N. Vinogradov, Chem. Rev. 96 (1996) 3113–3124.

[2] S.N. Vinogradov, P.K. Sharma, A.N. Qabar, J.S. Wall, J.A. Westrick, J.H. Simmons, S.J. Gill, J. Biol. Chem. 266 (1991) 13091–13096.

[3] P.K. Sharma, A.R. Kuchumov, R. Chottard, P.D. Martin, J.S. Wall, S.N. Vinogradov, J. Biol. Chem. 271 (1996) 8754–8762.

[4] S.N. Vinogradov, S.D. Lugo, M.G. Mainwaring, O.H. Kapp, A.V. Crewe, Proc. Natl. Acad. Sci. USA 83 (1986) 8034–8038.

[5] P.D. Martin, A.R. Kuchumov, B.N. Green, R.W.A. Oliver, E.H. Braswell, J.S. Wall, S.N. Vinogradov, J. Mol. Biol. 255 (1996) 154–169.

[6] M. Schatz, E. Orlova, P. Dube, J. Jäger, M. Van Heel, J. Struct. Biol. 114 (1995) 28–40.

[7] F. De Haas, A.R. Kuchumov, S.N. Vinogradov, J.N. Lamy, Biochemistry 36 (1997) 7330–7338.

[8] F. De Haas, J.-C. Taveau, N. Boisset, O. Lambert, S.N. Vinogradov, J.N. Lamy, J. Mol. Biol. 255 (1996) 140–163.

[9] F. De Haas, J.-C. Taveau, N. Boisset, O. Lambert, S.N. Vinogradov, J.N. Lamy, Biophys. J. 70 (1996) 1973–1984.

[10] F. De Haas, F. Zal, F.H. Lallier, A. Toulmond, J.N. Lamy, Proteins 26 (1996) 241–256.

[11] F. De Haas, F. Zal, V. You, F. Lallier, A. Toulmond, J.N. Lamy, J. Mol. Biol. 264 (1996) 111–120.

[12] S.N. Vinogradov, P.K. Sharma, Meth. Enzymol. 231 (1994) 112–124.

[13] H. Pauly, L. Packer, H.P. Schwan, J. Biophys. Biochem. Cytol. 4 (1963) 589–601.

[14] P. Debye, Polar Molecules, Dover Pub., New York, 1929.

[15] S. Takashima, Electrical Properties of Biopolymers and Membranes, Adam Hilger, London, UK, 1989, ch. 5.

[16] J.J. Oncley, in: E.J. Cohn, J.T. Edsall (Eds.), Proteins, Peptides and Amino Acids, Reinhold Publishing, New York, NY, 1943, ch. 22.
[17] J.T. Edsall, Proteins, Peptides and Amino Acids, Reinhold Publishing, New York, NY, 1945, pp. 506–517.
[18] J.T. Edsall, J. Wyman, Biophysical Chemistry, Academic Press, New York, NY, 1958, ch. 6.
[19] S.N. Vinogradov, O.H. Kapp, M. Ohtsuki, in: J. Harris (Ed.), Electron Microscopy of Proteins, vol. 3, Academic Press, New York, NY, 1982, pp. 135–163.
[20] A. Krebs, A.R. Kuchumov, P.K. Sharma, E.H. Braswell, P. Zipper, R.E. Weber, R. Chottard, S.N. Vinogradov, J. Biol. Chem. 271 (1996) 18695–18704.
[21] P.D. Martin, K.L. Eisele, M.A. Doyle, A.R. Kuchumov, D.A. Walz, E. Arutyunyan, S.N. Vinogradov, B.F.P. Edwards, J. Mol. Biol. 255 (1996) 170–175.
[22] K.S. Cole, R.H. Cole, J. Chem. Phys. 9 (1941) 341–351.
[23] R. Verbruggen, V. Blaten, M.Y. Rosseneu-Motreff, H. Peeters, in: H. Peeters (Ed.), Protides of the Biological Fluids, Pergamon Press, New York, NY, 1969.
[24] M.Y. Rosseneu-Motreff, F. Soetewey, R. Lamote, H. Peeters, Biopolymers 10 (1971) 1039–1040.
[25] S. Takashima, Biophys. J. 64 (1993) 1550–1561.
[26] S. Takashima, K. Asami, Biopolymers 25 (1993) 1717–1733.
[27] E. Fredericq, C. Houssier, Electric Dichroism and Electric Birefringence, Clarendon Press, Oxford, UK, 1973.
[28] D. Porschke, Biophys. Chem. 28 (1987) 137–147.
[29] D.J. Barlow, J. Thornton, Biopolymers 25 (1986) 1717–1733.
[30] J. Antosiewicz, Biophys. J. 69 (1995) 1344–1354.
[31] S. Takashima, Recent Res. Dev. Phys. Chem. 1 (1997) 143–164.
[32] D. Porschke, Biophys. Chem. 66 (1997) 241–257.
[33] J.G. Kirkwood, J.B. Shumaker, Proc. Natl. Acad. Sci. USA 38 (1952) 855–858.
[34] S. Takashima, J. Polymer Sci. 56 (1962) 257–265.
[35] S.C. Blacklow, P.S. Kim, Nature Struct. Biol. 3 (1996) 758–761.
[36] D. Fass, S. Blacklow, P.S. Kim, J.M. Berger, Nature 388 (1997) 691–693.
[37] A.M. Friedman, T.O. Fischmann, T.A. Steitz, Science 268 (1995) 1721–1727.
[38] M. Lewis, G. Chang, N.C. Horton, M.A. Kercher, H.C. Pace, M.A. Schumacher, R.G. Brennan, P. Lu, Science 271 (1996) 1247–1254.
[39] D. Porschke, K. Tovar, J. Antosiewicz, Biochemistry 27 (1988) 4674–4679.